Biochimica et Biophysica Acta 1865 (2017) 20–27

Contents lists available at ScienceDirect

Biochimica et Biophysica Acta

journal homepage: www.elsevier.com/locate/bbapap

Controlled lid-opening in *Thermomyces lanuginosus* lipase– An engineered switch for studying lipase function

Jakob Skjold-Jørgensen [a,b], Jesper Vind [b], Olga V. Moroz [c], Elena Blagova [c], Vikram K. Bhatia [b], Allan Svendsen [b], Keith S. Wilson [c,*], Morten J. Bjerrum [a,*]

[a] Department of Chemistry, University of Copenhagen, Universitetsparken 5, DK-2100 Copenhagen Ø, Denmark
[b] Novozymes A/S, Brudelysvej 35, DK-2880 Bagværd, Denmark
[c] York Structural Biology Laboratory, Department of Chemistry, The University of York, York YO10 5DD, UK

ARTICLE INFO

Article history:
Received 18 April 2016
Received in revised form 9 September 2016
Accepted 26 September 2016
Available online 28 September 2016

Keywords:
TlL, *Thermomyces lanuginosus* lipase
QCM-D, quartz crystal microbalance with dissipation monitoring
Intrinsic switch
Interfacial activation
Lid
Interfacial binding
Crystal structure

ABSTRACT

Here, we present a lipase mutant containing a biochemical switch allowing a controlled opening and closing of the lid independent of the environment. The closed form of the TlL mutant shows low binding to hydrophobic surfaces compared to the binding observed after activating the controlled switch inducing lid-opening. We directly show that lipid binding of this mutant is connected to an open lid conformation demonstrating the impact of the exposed amino acid residues and their participation in binding at the water-lipid interface. The switch was created by introducing two cysteine residues into the protein backbone at sites 86 and 255. The crystal structure of the mutant shows the successful formation of a disulfide bond between C86 and C255 which causes strained closure of the lid-domain. Control of enzymatic activity and binding was demonstrated on substrate emulsions and natural lipid layers. The locked form displayed low enzymatic activity (~10%) compared to wild-type. Upon release of the lock, enzymatic activity was fully restored. Only 10% binding to natural lipid substrates was observed for the locked lipase compared to wild-type, but binding was restored upon adding reducing agent. QCM-D measurements revealed a seven-fold increase in binding rate for the unlocked lipase. The TlL_locked mutant shows structural changes across the protein important for understanding the mechanism of lid-opening and closing. Our experimental results reveal sites of interest for future mutagenesis studies aimed at altering the activation mechanism of TlL and create perspectives for generating tunable lipases that activate under controlled conditions.

1. Introduction

Lipases, such as the lipase from *Thermomyces lanuginosus*, catalyze the hydrolysis of triglycerides (TAG) at the water-lipid interface producing mono- and di-glycerides and free fatty acids (FFA). These enzymes are part of the alpha/beta-hydrolase fold family and contain an active site triad (Ser, Asp and His) similar to that found in serine proteases [1]. Due to the innate ability of lipases to function at high temperatures, alkaline pH, in organic solvents and at low water activities the use of lipases as industrial biocatalysts is wide-spread and includes applications within detergents, baking, fuel, fine chemicals, paper and leather [2–5]. One of the characteristic traits of TlL and related lipases is the low activity displayed on water soluble, monomeric substrates in homogenous aqueous solution. As the substrate concentration increases and exceeds its critical micelle concentration (CMC), the activity increases many-fold [6]. This phenomenon is referred to as "interfacial activation" and besides an aggregation of the substrate it implicates a structural change in the enzyme itself [1,7–9], involving a repositioning of an α-helix (residues 86–93) bounded by two hinges, residues 82–85 and 94–98. This structural unit called the lid (or flap) covers the active site in the enzyme's inactive state. Upon activation, the lid changes conformation in a rigid body hinge-type movement, exposing the active site triad Ser146, Asp201 and His258 which enables substrate access and initiation of catalysis. The lid is highly amphipathic, containing a distinctive distribution of hydrophobic and hydrophilic residues [7]. In the closed state, hydrophilic residues are exposed at the surface of the protein making favorable interactions with the polar solvent. In the active state, lid-opening exposes the hydrophobic residues to the solvent which act as "lipid anchors", positioning the enzyme correctly for catalysis at the water-lipid interface [10–12]. Indeed, as suggested by several theoretical and experimental studies, lid opening is induced in apolar solvents of low dielectric constant [10,12–20] and results in the exposure of a combined ~750 Å^2 hydrophobic surface area [7],

Abbreviations: CMC, critical micelle concentration; pNP, para-nitrophenol; QCM-D, quartz crystal microbalance with dissipation monitoring; TCEP, Tris (2-Carboxyethyl) phosphine.

* Corresponding authors.
E-mail addresses: keith.wilson@york.ac.uk (K.S. Wilson), mobj@chem.ku.dk (M.J. Bjerrum).

http://dx.doi.org/10.1016/j.bbapap.2016.09.016
1570-9639/

corresponding to the area around the active site pocket. Although the activation mechanism of lipases has been studied for decades much remains unknown as to how changing the activation mechanism can improve its function in industrial applications. In this study, we set out to create a TlL mutant for which activity and interfacial binding could be directly controlled by a tunable lid. Accordingly, we engineered a pair of cysteine residues into the backbone of TlL. Here, we show that the mutant, referred to as TlL_locked, with mutations at I255C and I86C, contains a functional activity-switch enabling direct control of substrate access to the active site and binding to substrate surfaces. The choice of a disulfide bond as chemical lock was based on its biochemical nature. Disulfide bonds in proteins convey general structural stability by influencing the thermodynamics of protein folding, reducing structural fluctuations [21]. In addition, they commonly make the native state more compact thus rendering the molecule less susceptible to proteolysis or chemical denaturation [22]. Wild type TlL contains three disulfide bonds, C22-C268, C104-C107, C36-C41 which help to explain its high thermal and kinetic stability in oxidative environments [5,24]. Furthermore, disulfide bonds have earlier been used for protein engineering purposes to impact enzymatic activity as demonstrated by Matsumura et al. [23]. In a recent study [51] a disulfide bond was introduced into *Malassezia globosa* lipase between position 106 and 233 (L106C/V233C) affecting the movement of the lid. The mutant had nearly full activity when reduced but the activity was hampered when the disulfide bond was formed indicating that full activation of the lipase requires full mobility of the lid.

Successful formation of the switch in TlL_locked was confirmed by the crystal structure of the variant, revealing a closed and somewhat strained lid conformation. To assess the impact of the disulfide bond on protein stability, a thermal melt assay was used to show that thermo-stability of TlL_locked is decreased compared to wild-type. Although the lid is closed, investigation of structural characteristics around the lid-region suggests that TlL_locked rests in a pre-activated state. The impact of the disulfide bond on enzymatic activity was assessed on short, medium and long-chain ester substrates emulsified in non-ionic surfactant or embedded in lipid layers of rendered porcine fat and olive oil. Furthermore, the lid's role in interfacial binding to natural substrates and hydrophobic surfaces was investigated using a micro-titer plate set-up and quartz crystal microbalance with dissipation (QCM-D) analysis, respectively.

2. Materials and methods

2.1. Materials

Unless otherwise stated, all reagents and biochemical supplies were purchased from Sigma Aldrich and affiliates.

2.2. Engineering and nomenclature of lipase mutants

An intrinsic activity switch was grafted into TlL by single site mutations I86C and I255C enabling disulfide bond formation locking the lipase lid in its closed state. This variant is referred to as TlL_locked. Also, single cysteine mutant controls, C86 (TlL_C86) and C255 (TlL_C255) were made.

2.3. Variant construction, transformation and screening

The genetic variants were created by single site mutagenesis [52]. DNA was sequenced across the whole gene and transformed into an *Aspergillus oryzae* strain and fermented according to previous protocols [25]. Protoplasts were stored at −80 °C and thawed when needed. Expression was verified by running SDS-page analysis SimplyBlue Safestain (Life Technologies, catalog no. LC6065). Variant screening was carried out for successfully transformed *Aspergillus oryzae* strains using a standard pNP-valerate activity assay [26].

2.4. Protein purification

Fermentation broths were sterile filtered using filter units (Nalgene) with appropriate filters (CAT No.: 1820-090, WHATMAN). NaCl was added to filtered supernatant to a final concentration of 1 M. The protein purifications were carried out using an ÄKTA Prime (Amersham Biosciences) according to a previous protocol [27]. Variants were purified to a high degree with no observable contaminations verified by SDS-page using Simply Blue Safestain (Life Technologies, catalog no., LC6065). All samples were buffer-exchanged and concentrated in 50 mM MOPS pH 7.5 using centrifugal filter units (Ultracel-10K, Millipore). Purification of the control mutant, TlL_C86, failed, which was ascribed to low expression yields and high degree of binding to the column during purification.

2.5. Intact molecular mass analysis

This was carried out for TlL_locked by LC-ESI-MS analysis using a MAXIS II electrospray mass spectrometer (Bruker Daltonik GmbH, Bremen, DE). All samples were diluted to ~0.5 mg/mL in MilliQ water. The intact molecular masses were determined for untreated samples and samples treated with 1 mM TCEP. Samples were incubated for 30 min before being applied to an Aeris Widepore C4 column (Phenomenex), washed and eluted running an acetonitrile linear gradient and introduced to the electrospray source with a flow of 300 mL/min by an Ultimate 3000 LC system (Dionex). Data analysis was performed with DataAnalysis version 4.2 (Bruker Daltonik GmbH, Bremen, DE). Intact molecular masses of the untreated and reduced samples are shown in Fig. S1 and Table S1, Supporting Information.

2.6. pNP-ester emulsion assay

The activity towards short and medium chain pNP-ester substrates, pNP-butyrate and pNP-decanoate, respectively, was determined in 50 mM Tris + 10 mM $CaCl_2$ + 0.4% (v/v) Triton X-100 (CMC is 0.015% (v/v) [28]) (substrate buffer). Tris (2-Carboxyethyl) phosphine (TCEP) was added as reducing agent in the concentration range of 0–10 mM. 10 μL enzyme solution was mixed with 190 μL substrate buffer. The increase in absorbance at 405 nm due to released pNP-moiety was measured over 5 min and specific activity was determined from steepest slope. The final lipase concentration was 2 μg/mL.

2.7. Lipase activity

This was determined according to a previous protocol [29]. Two sets of substrate-coated 96 well micro-titer assay plates were made 1) olive oil + pNP-decanoate and 2) rendered porcine fat (lard) + pNP-palmitate, respectively (in a 1:1 molar ratio). 190 μL buffer (100 mM Tris pH 8 + 2 mM $CaCl_2$ with or without 5 mM TCEP) was added to 10 μL protein sample (50 μg/mL) in non-binding plates (Corning, catalog no. 3995) to minimize unspecific adsorption of lipase to the well surface. Plates were subsequently incubated for 10 min at room temperature. Using a multi-pipette (Liquidator RAININ), 150 μL was transferred to the assay plate and the increase in absorbance at 405 nm due to released pNP-moiety was measured over 10 min and the activity was determined from steepest slope.

2.8. Steady state fluorescence spectroscopy

Intrinsic tryptophan fluorescence emission spectra were recorded on a fluorescence spectrometer at room temperature (PerkinElmer, LS50B) in a quartz cuvette (Hellma QS 105.250). Emission was detected between 310 and 650 nm with excitation at 295 nm. Excitation and emission slit-widths were 4 nm and 12 nm, respectively. The scan-rate was 50 nm/min and an average of two consecutive measurements were taken. Emission spectra were measured in two different buffers

e.g. A) 25 mM MOPS pH 7.5 and B) 25 mM MOPS pH 7.5 + 0.4% (v/v) Triton X-100 + 1 mM TCEP. Note, the Triton X-100 used (Cas. No. 93422) was a reduced form, suitable for fluorescence measurements with approximately the same CMC as the oxidized Triton X-100 (0.25 mM vs. 0.22 mM, respectively [30]). Changes in fluorescence emission intensity over time were measured by conducting emission scans every 4 min for 30 min. Final scans were taken after 65 min.

2.9. Binding to natural, triglyceride substrates

Differences in binding to lipid layers of natural substrates, e.g. olive oil and lard, were investigated in a set-up similar to the lipase assay described above, but without pNP-substrate. Samples were diluted to 50 μg/mL in 25 mM MOPS pH 7.5. 190 μL buffer (100 mM Tris pH 8 + 2 mM $CaCl_2$) with and without 1 mM TCEP were added to 10 μL sample in a non-binding micro-titer plate (Corning). After incubation for 10 min at room temperature, 150 μL of the sample volume was added to a micro-titer plate coated with 100 nmol olive oil or lard. Binding of lipase to the olive or lard lipid surfaces was determined by the residual activity measured as the activity in the supernatant over time (between 2 and 40 min) relative to the initial activity at time zero. 20 μL supernatant was assayed in a 100 μL 50 mM Tris pH 7.5 + 0.4% Triton X-100 + 10 mM $CaCl_2$ reaction buffer calculating activity from the initial rate of pNP-butyrate hydrolysis at 405 nm.

2.10. QCM-D analysis of lipase binding

Lipase binding experiments were carried out on a E4 quartz crystal microbalance with dissipation instrument (QCM-D (Q-Sense, Sweden)) with temperature control and a peristaltic pump ensuring controlled flow rate. Binding was carried out on standard hydrophobic surfaces, created as alkanethiol ($HS(CH_2)_{15}CH_3$) surface assembled monolayer (SAM) on the Au sensor crystals [31,32]. The buffer used was a 50 mM HEPES (pH 7.5), 100 mM NaCl, 1 mM $CaCl_2$ made with MilliQ water subsequently filtered (0.22 μm) and degassed. Lipase binding was monitored at 5 μM recording frequency and dissipation changes for 5 harmonics (overtones n = 3, 5, 7, 9 & 11). For all samples, the values of Δf for all overtones were similar and with small dissipation values, thus the adsorbed protein mass was calculated according to the Sauerbrey equation [33], converting Δf into mass in ng/cm^2. The temperature was maintained at 22 °C and raw data were analyzed with Q-tools software and fitted for kinetics with single exponential decay function using Igor Pro (Wavemetrics Inc.).

2.11. Thermal stability

SYPRO Orange™ (SO) (CAT# S5692, 5000× stock concentrate) was diluted 250× in 50 mM MOPS, pH 7.5. Protein samples were diluted to 0.1 mg/mL. 15 μL of SO and protein solution was added to a final volume of 30 μL to a white 96 well MTP (Eurogentec RT-PL96-AFW), reaching a final protein concentration of 0.1 mg/mL (3 μM). The plate was sealed with an optical PCR seal (Eurogentec RT-OPSL 100). Melting curves for each variant were determined (StepOnePlus Real Time PCR System, Applied Biosystems) running a temperature gradient from 25 °C to 96 °C at a scan-rate of 76 °C pr/h and with an initial 15 minute reaction time at 25 °C.

2.12. Crystallization and data collection

The protein was additionally EndoH treated prior to crystallization using a deglycosylation kit from New England BioLabs (catalog number P0702L). The protein to EndoH ratio was 10:1, and was incubated at 37 °C overnight in the presence of G5 reaction buffer (50 mM sodium citrate pH 5.5). Initial crystallization screening was carried out using sitting-drop vapor-diffusion with drops set up using a *Mosquito Crystal* liquid handling robot (TTP LabTech, UK) with 150 nL protein solution plus 150 nL reservoir solution in 96-well format plates (MRC 2-well crystallization microplate, Swissci, Switzerland) equilibrated against 54 μL reservoir solution. Crystallization trays were placed in a Rigaku Minstrel HT-UV imaging system for storage and inspection. Experiments were carried out at two temperatures, 4 °C and 20 °C, with a number of commercial screens. The best diffraction quality crystals were obtained at 20 °C in JCSG A1 (50% PEG400, 0.2 M lithium sulfate, 0.1 M Na-acetate pH 4.5). Data to 1.8 Å were collected at the Diamond Light Source beamline I04.

2.13. Structure solution and refinement

All computations were carried out using programs from the CCP4 suite [34] unless otherwise stated. The data were processed with XDS [35]. The space group was $P4_32_12$; a = b = 90.48 Å; c = 160.46 Å. The structure was solved by MOLREP [36] with the structure of wild-type TlL (PDB entry; 1DT3 [28]) as a search model. The structure was refined using *REFMAC* [29], iterated by manual model building/correction in *COOT* [37] and validated using MOLPROBITY [38]. Processing and refinement statistics are given in Table S2, Supporting Information. Structure figures were prepared using CCP4mg [39]. Coordinates and structure factors have been deposited in the Protein Data Bank (accession number 5ap9).

3. Results and discussion

3.1. Enzymatic activity of TlL_locked is restored in substrate emulsions and on a set of natural lipid substrate surfaces upon adding reducing agent

Enzymatic activity of wild-type TlL and TlL_locked was determined towards pNP-decanoate emulsified in Triton X-100 as a function of TCEP concentration (Fig. 1A). The activity of TlL was nearly unchanged (around 150 μmol/min/mg) throughout the applied TCEP concentration range of 0–10 mM. In contrast, TlL_locked displayed very low activity (~2–5 μmol/min/mg) in the absence of TCEP indicating restricted access of the substrate to the active site. As the concentration of TCEP increased, a concomitant increase in activity was observed reaching wild-type levels at 10 mM TCEP. A similar activity-increase was observed on short chained pNP-butyrate (see Fig. S3, Supporting Information) for TlL_locked as a function of TCEP concentration. The molecular mass of TlL_locked after treatment with around 300× molar excess of TCEP for 30 min at room temperature (pH 7.5) was two units lower than untreated TlL_locked corresponding to a single reduced disulfide bond (Fig. S1 and Table S1, Supporting Information). Hence, these results indicate a specific reduction of the C86-C255 disulfide bond with the other three disulfides left unaffected.

The activity towards pNP-decanoate and pNP-palmitate embedded in a lipid layer of olive oil and lard, respectively, was determined as previously described (Fig. 1B) [29]. In the absence of reducing agent, the activity of TlL_locked was low (2 μmol/min/mg and 0.5 μmol/min/mg). As TCEP was added to the buffer, the enzymatic activity of TlL_locked increased nearly 10-fold indicating full recovery of enzymatic activity compared to wild-type and single cysteine mutant, TlL_C255 (Supporting Information, Fig. S5). These results clearly demonstrate the key role of the lid in controlling enzymatic activity and interfacial activation as supported by previous studies [29,40–45].

3.2. The lid mediates binding of TlL to substrate surfaces

The binding of TlL and TlL_locked to lipid surfaces of olive oil and lard was investigated by measuring the residual activity in the supernatant as a function of time at pH 8 in the absence of reducing agent (Fig. 2). For TlL, the fraction of bound molecules reached ~50% after 40 min on both olive oil and lard with and without TCEP in the buffer solution. For untreated TlL_locked the bound fraction was very low on olive oil and lard (~10%) after 40 min of incubation. As TCEP was

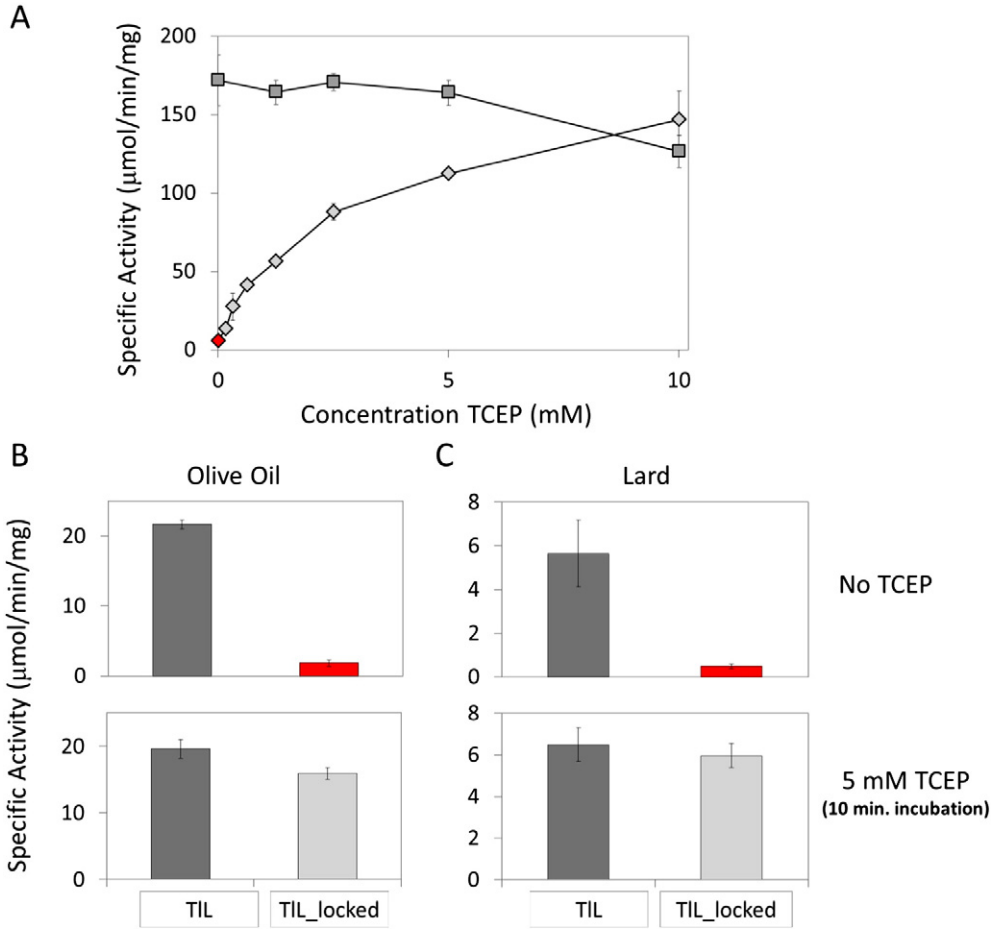

Fig. 1. Enzymatic activity of TlL and TlL_locked. A) Specific activity (μmol/min/mg) towards pNP-decanoate emulsified in 0.4% Triton X-100 as a function of TCEP concentration of TlL (dark grey and blue squares, black line) and TlL_locked (red and light grey diamonds, black line). The error bars denote the standard deviation from triplicate measurements at room temperature. This assay was also carried out with pNP-butyrate as substrate, see Supporting Information, Fig. S3. Lipase activity was measured towards pNP–decanoate and pNP-palmitate embedded in a lipid layer of B) olive oil and C) lard at pH 8 for TlL (dark grey columns) and TlL_locked (red and light grey columns). Activity was determined in 100 mM Tris + 2 mM $CaCl_2$ with and without 5 mM TCEP. Assay was run for 20 min at room temperature and activity was calculated from steepest slope of the increase in absorbance of the pNP-moiety at 405 nm. The error bars denote the standard deviation from triplicate measurements.

added to the buffer, TlL_locked displayed binding profiles similar to wild-type on both lipid substrates with ~50% bound fraction after 40 min.

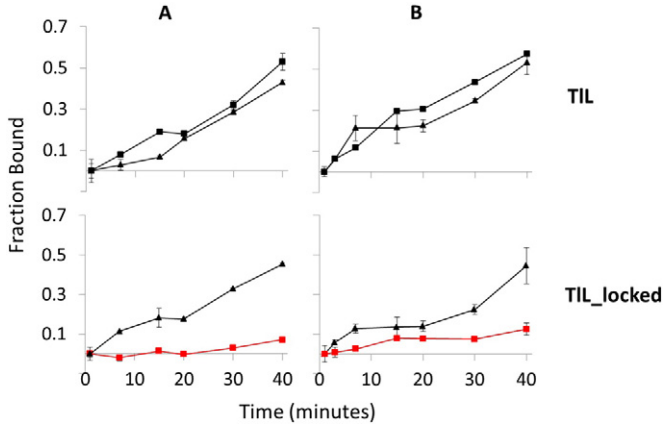

Fig. 2. Amount of bound lipase as a function of time to A) olive oil and B) lard, determined from the residual lipase activity in the supernatant determined at different time points. Binding was investigated in buffers with (triangles) and without (squares) reducing agent, TCEP. Untreated TlL_locked is highlighted with red line. Buffers used were: 100 mM Tris pH 8 + 2 mM $CaCl_2$ and 100 mM Tris pH 8 + 2 mM $CaCl_2$ + 1 mM TCEP. Error bars denote the standard deviation from triplicate.

3.3. Time dependent un-locking of locked TlL observed using intrinsic tryptophan fluorescence

As shown previously, Trp89 in the lid of TlL is responsible for more than 60% of the protein's total fluorescence emission [46]. Accordingly, the steady state fluorescence emission spectra of TlL and TlL_locked were measured to investigate the microenvironment around Trp89. In buffer alone (no surfactant or reducing agent) the Trp fluorescence emission spectrum for TlL_locked was slightly blue-shifted with an emission maximum at 336 nm compared to 339 nm for wild-type (Supporting Information Fig. S6). In addition, the fluorescence intensity was quenched (~30% relative to wild-type). As described by Cowgill, thiol groups and disulfide bonds act as strong quenchers of tryptophan and tyrosine fluorescence in proteins [47]. We therefore ascribed this high degree of quenching to the successfully formed disulfide bond. Accordingly, in order to investigate lid-opening (activation) of TlL_locked the fluorescence emission spectra were measured over time in the buffer used in the activity assay containing non-ionic detergent, Triton X-100 and TCEP (Fig. 3). As the detergent concentration in this buffer was several fold higher than the CMC (~0.015% v/v) the emission spectrum of wild-type likely represents the Trp environment of an open lid conformation in accordance with previous studies [48].

For TlL_locked, the degree of intrinsic Trp quenching (~30%) was unchanged in this buffer (Fig. 3A) relative to wild-type indicating that the disulfide bond was unaffected by the presence of detergent micelles.

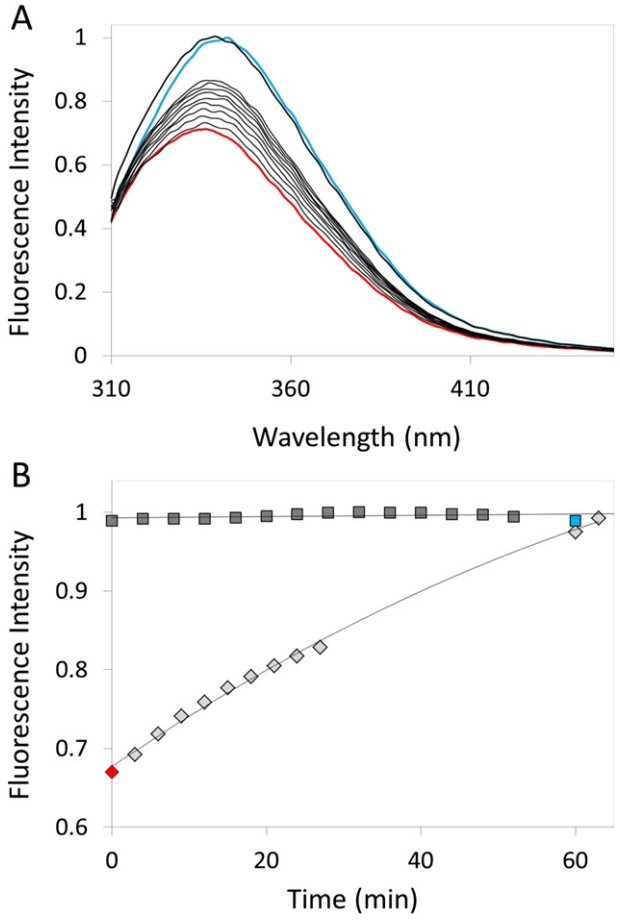

Fig. 3. A) Tryptophan fluorescence emission spectra of TlL_locked (red line) normalized to the emission intensity of wild-type TlL (blue line). Emission scans were taken every 4 min (black lines) for 30 min and final scans after 65 min (black line) in 25 mM MOPS +2 mM CaCl2 + 0.4% Triton X-100 containing 1 mM TCEP at 22 °C. B) The integrated fluorescence emission intensity plotted as a function of time for TlL_locked (red and black diamonds) and TlL (blue squares). A polynomial and a line were fitted to the data-points for TlL_locked and wild-type, respectively.

As TCEP was added, lid-opening of TlL_locked was measured over time with emission spectra taken over the course of 65 min. As seen, the fluorescence emission spectrum gradually underwent a red-shift and an increase in fluorescence intensity, ultimately reaching the same fluorescence intensity as wild-type after 65 min of incubation (Fig. 3B). Hence, these experiments indicate that reduction of the disulfide bond and concomitant lid-opening occurs in TlL_locked as TCEP is added to solution.

3.4. Interfacial binding is impaired for TlL_locked, but is partially restored under reducing conditions revealed by QCM-D analysis

QCM-D is a useful tool for real-time detection of biomolecule adsorption to solid/liquid interfaces and was here employed to evaluate the adsorption traits of TlL and TlL_locked to a hydrophobic surface (Fig. 4). The observed changes in resonance frequency (Δf) for TlL reflect adsorbed lipase mass to the hydrophobic surface and were in good agreement with previous studies [31] (Fig. 4A). For each sample, the values of Δf for all overtones (n = 5, 7, 9) were similar (Fig. 4A and C) with small dissipation value changes enabling the adsorbed protein mass to be calculated according to the Sauerbrey equation. The measured equilibrium protein density was 315 ng/cm^2 and corresponded well with a hydrated dense monolayer of enzyme (Fig. 4B) [31].

In addition, the overlapping frequency overtones and the small dissipation values confirmed a thin homogenous monolayer of bound lipase. Notably, binding for TlL_locked was severely impaired displaying a slower binding rate and equilibration density at the hydrophobic surface ascribed to the closed lid conformation preventing the large hydrophobic surface area around the active site to become exposed. Switching the locked lipase open with a reducing agent caused the binding rate to increase seven-fold reaching the same Δf levels as wild-type TlL indicative of a similar binding mode (Fig. 4D). These results suggest that the full hydrophobic surface area on the lipase upon lid-opening is critical for lipase binding kinetics and equilibrium densities. Although the binding rate increased for TlL_locked in the presence of TCEP, the rate was not 100% restored, indicating that the mutations, I86C and I255C, likely play a key role in interfacial binding. Indeed, as previously proposed, these residues serve as hydrophobic anchors positioning the lipase correct for catalysis [11].

The results from the activity and binding assays suggest that the switch created in TlL_locked enables both control over interfacial binding and enzymatic activity. These findings highlight the lid's importance in mediating surface adsorption and clearly show that the open form of the lid represents a major lipid binding region of the enzyme. The proposal that binding and catalysis are interdependent processes, governed by the exposure of the hydrophobic patch around the active site and subsequent penetration of hydrophobic residues of the lid into the lipid layer is hereby experimentally confirmed.

3.5. The crystal structure of TlL_locked shows formation of an intrinsic switch with hydrophobic anchors buried in the active site pocket

From structural visualization of inactive TlL (PDB entry; 1DT3) using PyMol [33] residues I255 and I86 were selected as suitable sites for cysteine mutagenesis and successful formation of a disulfide bond spanning the active site pocket. Notably, the obtained crystal structure showed the presence of the engineered disulfide bridge, and the B-values furthermore reveal that the lid residues, 83–98, were less ordered than the surrounding region (Fig. S2, Supplementary Information). These results indicate that the forced closed structure of the variant causes some structural strain in the locked down lid.

The structure was aligned with those of the inactive (closed lid) and active (open lid) TlL (PDB entries; 1DT3 and 1EIN, respectively, Fig. 5A). It was evident that the overall structures were similar (alignment of C_α–atoms; TlL_locked vs. inactive TlL, rmsd = 0.335 and TlL_locked vs. active TlL, rmsd = 0.284). However, close inspection of the area around the lid-region revealed significant structural differences.

Previous studies on TlL have established the specific structural differences proposed to take place as the enzyme becomes activated at the water-lipid interface, based on a comparison of several crystal structures grown under different crystallization conditions [49]. It was concluded that three structurally different species of TlL are present at the lipid-water interface, which differ from one another in four structural phenomena defined here as the “lid-opening”, the “C-terminus swing”, the “α_1–helix crunch” and the “loop motion” (Fig. 5B).

Accordingly, going from a closed (inactive) to an open (activated) enzyme, a translocation of the C22-C268 disulfide bond occurs which causes the C-terminus to swing towards the α_1–helix creating a helix extension (crunch) (Fig. 5C). Furthermore, the loop behind the lid (residues 57–63), moves closer to the lid as it opens, stabilizing the open conformation. The crystal structure of TlL_locked showed successful formation of a disulfide bond between C255 and C86 causing the hinge domain anterior to the lid (H1) to stretch across the active site pocket which distorts the α–helix domain of the lid and locks the lid-region in a closed state, covering the active site triad (Ser146, Asp201 and His258). Moreover, as seen for active TlL, the C22-C268 disulfide bond in TlL_locked was in a *cis* conformation causing the C–terminus to swing towards the H1 region and creating the α_1–helix extension.

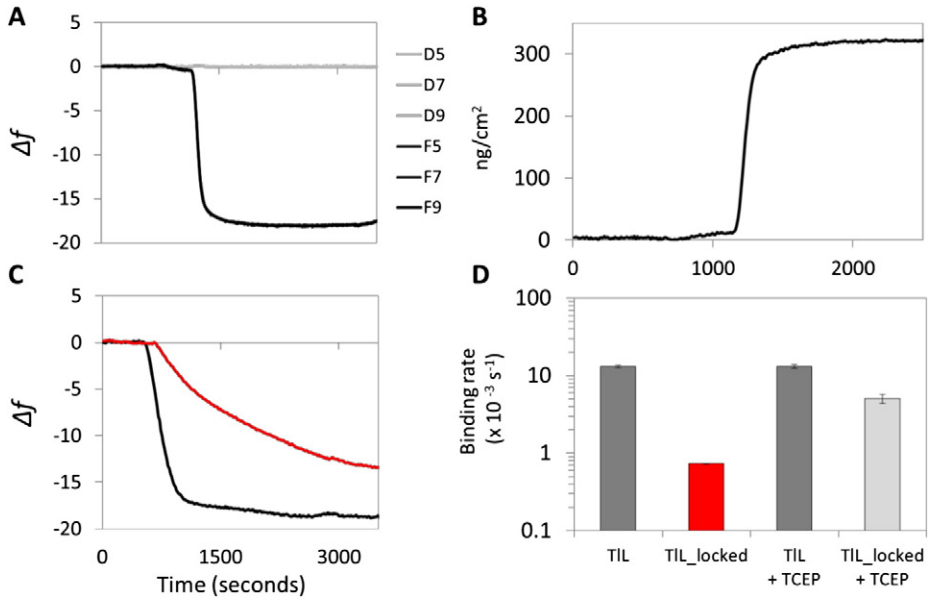

Fig. 4. A) Change in resonance frequency (Δf) and dissipation for adsorption of TIL on a hydrophobic surface at pH 7.5. Data are shown for overtones n = 5, 7, 9. B) Change in mass density as fitted to the Sauerbrey equation for TIL. C) Change in resonance frequency (Δf) for untreated TIL_locked (red curve) and reduced TIL_locked. D) Quantification of altered binding kinetics showing a semi-logarithmic plot of the binding rates extracted from Δf traces for TIL (dark grey), TIL_locked (red), TIL + TCEP (dark grey) and TIL_locked + TCEP (light grey), respectively. Error bars denote the standard error of the fit.

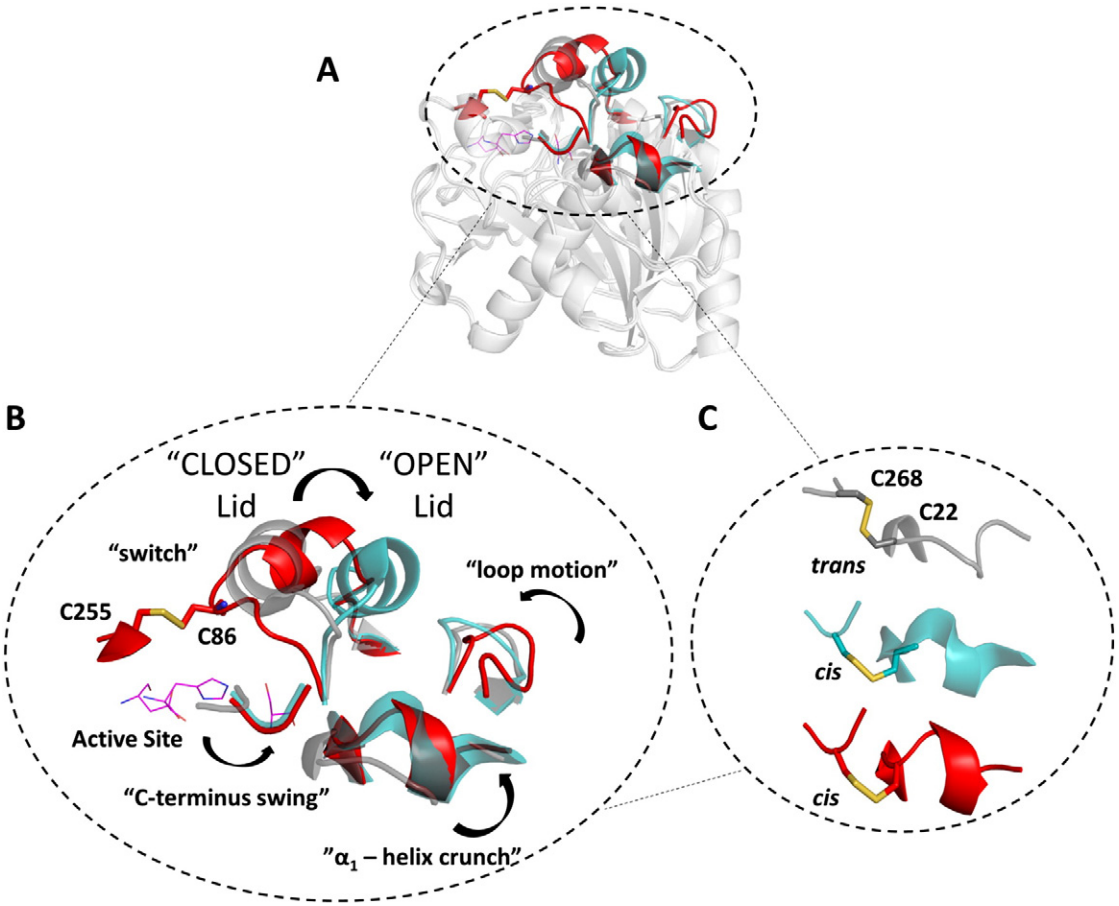

Fig. 5. A) Structural alignment of crystal structures from TIL_locked and inactive and active TIL (PDB entries; 1DT3 and 1EIN, respectively) (light grey cartoons). Major structural differences around the lid-region are highlighted within the dashed black circle (TIL_locked; red, inactive TIL; grey, active TIL; pale blue). B) Zoom-in on the major structural differences. TIL_locked contains a disulfide bond between residues C86 and C255, bridging the active site pocket, forcing the lid closed representing an intrinsic "switch". Four structural phenomena associated with lipase activation are highlighted i.e. the "lid-opening", "C-terminus swing", "α_1-helix crunch" and "loop motion". For inactive (closed) TIL, the C-terminus points outwards towards the solvent, while in TIL_locked and active (open) TIL, it swings towards the α_1 helix, in front of the lid-region creating an "α_1-helix crunch". The loop behind the lid moves closer to the lid as the lid opens as seen for active TIL. This is not evident in TIL_locked. C) The C-terminus swing and the α_1-helix crunch are caused by translocation of the C22—C268 disulfide bond from a *trans* to a *cis* conformation.

These structural features associated with lipase activation suggest that TlL_locked resides in a pre-activation state under the crystallization conditions used.

Interestingly, the loop (residues 57–62) in TlL_locked showed a distinct pull away from the lid-region compared to both inactive and active TlL ascribed to the strained, locked conformation of the lid. These results indicate that the movement of the lid and loop is interdependent of each other e.g. movement of the loop towards the lid occurs only when the lid opens. In light of this, our previous studies [29] support the notion that the loop moves closer to the lid upon activation. Here, a TlL mutant with a lid of both lipase and esterase residue composition showed successful formation of a disulfide bond between C86 (in the lid) and C62 (in the loop). The TlL mutant was more active on water-soluble substrates in homogenous, aqueous solution. This behavior is ascribed to an open lid conformation [29] where we have forced the loop and lid closer together.

3.6. Thermal stability

To build on the observation in the structure of a somewhat strained conformation induced by the disulfide bond (C86-C255) and supported by elevated temperature factors, we investigated the structural integrity of TlL_locked and of wild-type TlL using a thermal melt assay as previously described (see Supporting Information, Fig. S3). Importantly, the melting curves for both TlL and TlL_locked showed a sharp, single, distinct peak reflecting the homogeneity of the samples. The melting temperature of TlL_locked was 5 °C below that of wild type suggesting that the two mutations, I255C and I86C, and the disulfide bond between them, serve to destabilize the secondary structure. This is ascribed to energetically unfavorable structural restrictions imposed by the disulfide bond, having a negative impact on globular protein stability [50].

4. Conclusion

From analysis of the crystal structure and comparison between the inactive and active structures of wild-type TlL we propose that the engineered variant, TlL_locked, rests in a somewhat strained, pre-activated state under the crystallization conditions used. This was supported by the increased B-values of the lid-region. The crystal structure showed a successfully formed disulfide bond spanning the active site pocket, locking the lid in a closed conformation. Using a combination of activity and binding assays, we experimentally showed that this intrinsic bond enables control of both lipase activity and interfacial binding. These findings deepen the understanding of the structural changes important for lipase activation and the design approach behind TlL_locked has interesting ramifications for creating future lipases that are less prone to inhibition by substrate analogues and for enabling direct control of lipo-lytic activity. The variant described here could be used as a lipase probe for future studies. TlL_locked can be activated in seconds by chemical reduction when lipase activity is needed. Another possible use of this variant can be as a redox-switch lipase activated at low redox potential inside a cell.

Funding

This work was funded by the industrial PhD program EFU:Novozymes (12-128740 and 0604-01457B). We thank Diamond Light Source for access to beamline I04 (proposal number mx-9948) that contributed to the results presented here.

Transparency document

The Transparency document associated with this article can be found, in online version.

Acknowledgements

The authors would like to thank the scientists at Novozymes, R&D. Special thanks to Sisse Lakner Schmidt for technical assistance with QCM-D and Christian I. Jørgensen, Clive Owens and Peter R. Eriksen for technical guidance in mass spectrometry.

References

[1] L. Brady, A.M. Brzozowski, Z.S. Derewenda, E. Dodson, G. Dodson, S. Tolley, J.P. Turkenburg, L. Christiansen, B. Huge-Jensen, L. Norskov, A serine protease triad forms the catalytic centre of a triacylglycerol lipase, Nature 343 (1990) 767–770.
[2] S. Naik, A. Basu, R. Saikia, B. Madan, P. Paul, R. Chaterjee, J. Brask, A. Svendsen, Lipases for use in industrial biocatalysis: specificity of selected structural groups of lipases, J. Mol. Catal. B Enzym. 65 (2010) 18–23.
[3] K.-E. Jaeger, S. Ransac, B.W. Dijkstra, C. Colson, M. van Heuvel, O. Misset, Bacterial lipases, FEMS Microbiol. Rev. 15 (1994) 29–63.
[4] K.-E. Jaeger, M.T. Reetz, Microbial lipases form versatile tools for biotechnology, Trends Biotechnol. 16 (1998) 396–403.
[5] R.D. Schmid, R. Verger, Lipases: interfacial enzymes with attractive applications, Angew. Chem. Int. Ed. 37 (1998) 1608–1633.
[6] L. Sarda, P. Desnuelle, Action de la lipase pancréatique sur les esters en émulsion, Biochim. Biophys. Acta 30 (1958) 513–521.
[7] A. Brzozowski, U. Derewenda, Z. Derewenda, G. Dodson, D. Lawson, J. Turkenburg, F. Bjorkling, B. Huge-Jensen, S. Patkar, L. Thim, A model for interfacial activation in lipases from the structure of a fungal lipase-inhibitor complex, Nature 351 (1991) 491–494.
[8] U. Derewenda, A.M. Brzozowski, D.M. Lawson, Z.S. Derewenda, Catalysis at the interface: the anatomy of a conformational change in a triglyceride lipase, Biochemistry 31 (1992) 1532–1541.
[9] D.M. Lawson, A.M. Brzozowski, S. Rety, C. Verma, G.G. Dodson, Probing the nature of substrate binding in *Humicola lanuginosa* lipase through X-ray crystallography and intuitive modelling, Protein Eng. 7 (1994) 543–550.
[10] M.Ø. Jensen, T.R. Jensen, K. Kjaer, T. Bjørnholm, O.G. Mouritsen, G.H. Peters, Orientation and conformation of a lipase at an interface studied by molecular dynamics simulations, Biophys. J. 83 (2002) 98–111.
[11] A. Svendsen, Lipase protein engineering, Biochim. Biophys. Acta Protein Struct. Mol. Enzymol. 1543 (2000) 223–238.
[12] G.H. Peters, S. Toxvaerd, O. Olsen, A. Svendsen, Computational studies of the activation of lipases and the effect of a hydrophobic environment, Protein Eng. 10 (1997) 137–147.
[13] C.C. Gruber, J. Pleiss, Lipase B from *Candida antarctica* binds to hydrophobic substrate–water interfaces via hydrophobic anchors surrounding the active site entrance, J. Mol. Catal. B Enzym. 84 (2012) 48–54.
[14] S. Rehm, P. Trodler, J. Pleiss, Solvent-induced lid opening in lipases: a molecular dynamics study, Protein Sci. 19 (2010) 2122–2130.
[15] P. Trodler, R.D. Schmid, J. Pleiss, Modeling of solvent-dependent conformational transitions in *Burkholderia cepacia* lipase, BMC Struct. Biol. 9 (2009) 1.
[16] M. Norin, F. Haeffner, K. Hult, O. Edholm, Molecular dynamics simulations of an enzyme surrounded by vacuum, water, or a hydrophobic solvent, Biophys. J. 67 (1994) 548.
[17] M. Norin, O. Olsen, A. Svendsen, O. Edholm, K. Hult, Theoretical studies of *Rhizomucor miehei* lipase activation, Protein Eng. 6 (1993) 855–863.
[18] G.H. Peters, O. Olsen, A. Svendsen, R. Wade, Theoretical investigation of the dynamics of the active site lid in *Rhizomucor miehei* lipase, Biophys. J. 71 (1996) 119.
[19] L. Villo, A. Metsala, S. Tamp, J. Parve, I. Vallikivi, I. Järving, N. Samel, Ü. Lille, T. Pehk, O. Parve, *Thermomyces lanuginosus* lipase with closed lid catalyzes elimination of acetic acid from 11-acetyl-prostaglandin E2, ChemCatChem 6 (2014) 1998–2010.
[20] S. Santini, J.M. Crowet, A. Thomas, M. Paquot, M. Vandenbol, P. Thonart, J.P. Wathelet, C. Blecker, G. Lognay, R. Brasseur, L. Lins, B. Charloteaux, Study of *Thermomyces lanuginosa* lipase in the presence of tributyrylglycerol and water, Biophys. J. 96 (2009) 4814–4825.
[21] J. Thornton, Disulphide bridges in globular proteins, J. Mol. Biol. 151 (1981) 261–287.
[22] G. Bulaj, Formation of disulfide bonds in proteins and peptides, Biotechnol. Adv. 23 (2005) 87–92.
[23] M. Matsumura, W.J. Becktel, M. Levitt, B.W. Matthews, Stabilization of phage T4 lysozyme by engineered disulfide bonds, Proc. Natl. Acad. Sci. 86 (1989) 6562–6566.
[24] R. Fernandez-Lafuente, Lipase from *Thermomyces lanuginosus*: uses and prospects as an industrial biocatalyst, J. Mol. Catal. B Enzym. 62 (2010) 197–212.
[25] T. Christensen, H. Woeldike, E. Boel, S.B. Mortensen, K. Hjortshoej, L. Thim, M.T. Hansen, High level expression of recombinant genes in *Aspergillus oryzae*, Nat. Biotechnol. 6 (1988) 1419–1422.
[26] Vind, J. (2012) Constructing and screening a DNA library of interest in filamentous fungal cells. Google Patents
[27] E.M. Hedin, S.A. Patkar, J. Vind, A. Svendsen, K. Hult, P. Berglund, Selective reduction and chemical modification of oxidized lipase cysteine mutants, Can. J. Chem. 80 (2002) 529–539.
[28] S. Brocca, F. Secundo, M. Ossola, L. Alberghina, G. Carrea, M. Lotti, Sequence of the lid affects activity and specificity of *Candida rugosa* lipase isoenzymes, Protein Sci. 12 (2003) 2312–2319.
[29] J. Skjold-Jorgensen, J. Vind, A. Svendsen, M.J. Bjerrum, Altering the activation mechanism in *Thermomyces lanuginosus* lipase, Biochemistry 53 (2014) 4152–4160.

[30] G.E. Tiller, T.J. Mueller, M.E. Dockter, W.G. Struve, Hydrogenation of Triton X-100 eliminates its fluorescence and ultraviolet light absorption while preserving its detergent properties, Anal. Biochem. 141 (1984) 262–266.
[31] D. Otzen, Differential adsorption of variants of the *Thermomyces lanuginosus* lipase on a hydrophobic surface suggests a role for local flexibility, Colloids Surf. B: Biointerfaces 64 (2008) 223–228.
[32] L. Sun, K. Frykholm, L.H. Fornander, S. Svedhem, F. Westerlund, B.r. Åkerman, Sensing conformational changes in DNA upon ligand binding using QCM-D. Polyamine condensation and Rad51 extension of DNA layers, J. Phys. Chem. B 118 (2014) 11895–11904.
[33] M. Rodahl, B. Kasemo, On the measurement of thin liquid overlayers with the quartz-crystal microbalance, Sensors Actuators A Phys. 54 (1996) 448–456.
[34] M.D. Winn, C.C. Ballard, K.D. Cowtan, E.J. Dodson, P. Emsley, P.R. Evans, R.M. Keegan, E.B. Krissinel, A.G. Leslie, A. McCoy, Overview of the CCP4 suite and current developments, Acta Crystallogr. D Biol. Crystallogr. 67 (2011) 235–242.
[35] G.N. Murshudov, P. Skubák, A.A. Lebedev, N.S. Pannu, R.A. Steiner, R.A. Nicholls, M.D. Winn, F. Long, A.A. Vagin, REFMAC5 for the refinement of macromolecular crystal structures, Acta Crystallogr. D Biol. Crystallogr. 67 (2011) 355–367.
[36] A. Vagin, A. Teplyakov, Molecular replacement with MOLREP, Acta Crystallogr. D Biol. Crystallogr. 66 (2010) 22–25.
[37] P. Emsley, B. Lohkamp, W.G. Scott, K. Cowtan, Features and development of Coot, Acta Crystallogr. D Biol. Crystallogr. 66 (2010) 486–501.
[38] I.W. Davis, A. Leaver-Fay, V.B. Chen, J.N. Block, G.J. Kapral, X. Wang, L.W. Murray, W.B. Arendall, J. Snoeyink, J.S. Richardson, MolProbity: all-atom contacts and structure validation for proteins and nucleic acids, Nucleic Acids Res. 35 (2007) W375–W383.
[39] S. McNicholas, E. Potterton, K. Wilson, M. Noble, Presenting your structures: the CCP4mg molecular-graphics software, Acta Crystallogr. D Biol. Crystallogr. 67 (2011) 386–394.
[40] K.A. Dugi, H. Dichek, G.D. Talley, H.B. Brewer, S. Santamarina-Fojo, Human lipoprotein lipase: the loop covering the catalytic site is essential for interaction with lipid substrates, J. Biol. Chem. 267 (1992) 25086–25091.
[41] K.A. Dugi, H.L. Dichek, S. Santamarina-Fojo, Human hepatic and lipoprotein lipase: the loop covering the catalytic site mediates lipase substrate specificity, J. Biol. Chem. 270 (1995) 25396–25401.
[42] M. Martinelle, M. Holmquist, K. Hult, On the interfacial activation of *Candida antarctica* lipase A and B as compared with *Humicola lanuginosa* lipase, Biochim. Biophys. Acta (BBA)-Lipids and Lipid Metab. 1258 (1995) 272–276.
[43] M.L. Jennens, M.E. Lowe, A surface loop covering the active site of human pancreatic lipase influences interfacial activation and lipid binding, J. Biol. Chem. 269 (1994) 25470–25474.
[44] Z. Shu, M. Duan, J. Yang, L. Xu, Y. Yan, *Aspergillus niger* lipase: heterologous expression in *Pichia pastoris*, molecular modeling prediction and the importance of the hinge domains at both sides of the lid domain to interfacial activation, Biotechnol. Prog. 25 (2009) 409–416.
[45] Z. Shu, J. Wu, L. Xue, R. Lin, Y. Jiang, L. Tang, X. Li, J. Huang, Construction of *Aspergillus niger* lipase mutants with oil–water interface independence, Enzym. Microb. Technol. 48 (2011) 129–133.
[46] A. Stobiecka, S. Wysocki, A. Brzozowski, Fluorescence study of fungal lipase from *Humicola lanuginosa*, J. Photochem. Photobiol. B Biol. 45 (1998) 95–102.
[47] R.W. Cowgill, Fluorescence and protein structure: XI. Fluorescence quenching by disulfide and sulfhydryl groups, Biochim. Biophys. Acta Protein Struct. 140 (1967) 37–44.
[48] A. Jutila, K. Zhu, S.A. Patkar, J. Vind, A. Svendsen, P.K. Kinnunen, Detergent-induced conformational changes of *Humicola lanuginosa* lipase studied by fluorescence spectroscopy, Biophys. J. 78 (2000) 1634–1642.
[49] A.M. Brzozowski, H. Savage, C.S. Verma, J.P. Turkenburg, D.M. Lawson, A. Svendsen, S. Patkar, Structural origins of the interfacial activation in *Thermomyces* (*Humicola*) *lanuginosa* lipase, Biochemistry 39 (2000) 15071–15082.
[50] P.J. Hogg, Disulfide bonds as switches for protein function, Trends Biochem. Sci. 28 (2003) 210–214.
[51] S. Guo, G.M. Popowicz, D. Li, D. Yuan, Y. Wang, Lid mobility in lipase SMG1 validated using a thiol/disulfide redox potential probe, FEBS Open Bio 6 (2016) 477–483.
[52] M.P. Weiner, G.L. Costa, W. Schoettlin, J. Cline, E. Mathur, J.C. Bauer, Site-directed mutagenesis of double-stranded DNA by the polymerase chain reaction, Gene 151 (1994) 119–123.